J. Korean Inst. Electr. Electron. Mater. Eng.
Vol. 35, No. 4, pp. 348-352 July 2022
DOI: https://doi.org/10.4313/JKEM.2022.35.4.5
ISSN 1226-7945(Print), 2288-3258(Online)

Regular Paper

Resistive Switching Effects of Zinc Silicate for Nonvolatile Memory Applications

Minho Im, Jisoo Kim, Kyoungwan Park, and Junghyun Sok

Department of Physics, University of Seoul, Seoul 02504, Korea

(Received February 11, 2022; Revised February 22, 2022; Accepted March 16, 2022)

Abstract: Resistive switching behaviors of a co-sputtered zinc silicate thin film (ZnO and SiO_2 targets) have been investigated. We fabricated an Ag/$ZnSiO_x$/highly doped n-type Si substrate device by using an RF magnetron sputter system. X-ray diffraction pattern (XRD) indicated that the Zn_2SiO_4 was formed by a post annealing process. A unique morphology was observed by scanning electron microscope (SEM) and atomic force microscope (AFM). As a result of annealing process, 50 nm sized nano clusters were formed spontaneously in 200~300 nm sized grains. The device showed a unipolar resistive switching process. The average value of the ratio of the resistance change between the high resistance state (HRS) and the low resistance state (LRS) was about 10^6 when the readout voltage (0.5 V) was achieved. Resistance ratio is not degraded during 50 switching cycles. The conduction mechanisms were explained by using Ohmic conduction for the LRS and Schottky emission for the HRS.

Keywords: Resistive switching, Zinc silicate, Conduction mechanism

1. INTRODUCTION

With the development of the next generation memory devices, the resistive random access memory (ReRAM) has been considered as a promising candidate to replace the conventional memory devices due to its simple structure, high memory density, and low power consumption [1-6]. Since the resistive switching phenomenon was observed last half century, various materials have been studied for ReRAM application, such as transition metal oxides (Al_2O_3, ZnO, NiO, and TiO_2) [7,8], ferromagnetic materials ($Pr_{1-x}Ca_xMnO_3$, doped $SrZrO_3$, $SrTiO_3$) [9,10], and etc.

Zinc oxide (ZnO), a typical oxide semiconductor material with a wide bandgap (3.1~4 eV), has good transparency, moderate mobility, and the CMOS compatibility. In addition, ZnO thin films were widely investigated for ReRAM applications and revealed to have the memory properties of fast switching speed, large on/off ratio of resistance, stable endurance, and long retention. Recently, the resistive switching effect has been also observed in defective SiO_2 thin films, although silicon is not a transition metal [11-13]. SiO_2 ReRAM has poor I-V properties and ZnO ReRAM has high leakage current and low transparency compared to SiO_2. In this study, we use the zinc silicate as a new resistive switching material in order to complement shortcoming of each ZnO and SiO_2. Role of Zn atoms (particles) in SiO_x matrix attracted a considerable amount of attention.

2. EXPERIMENT

Zinc silicate thin film (ZnO and SiO_2 mixed film) was deposited on highly doped-Si (100) wafer by RF magnetron co-sputtering with ZnO and SiO_2 targets in an Ar atmosphere

✉ **Junghyun Sok; sokjh@uos.ac.kr**

at room temperature. The post thermal annealing process was performed to synthesize the zinc silicate film from ZnO and SiO_2 mixed film and crystallize it. The thickness of $ZnSiO_x$ thin film is estimated about 50 nm by ellipsometry. After annealing process, 5~6 nm size of decreasing was observed. For electrical measurement, Ag top electrode was deposited on zinc silicate thin film by thermal evaporation with the use of metal shadow mask of 300 μm diameter at ambient temperature. The highly doped-Si substrate was used for the bottom electrode. The current-voltage (I-V) characteristics of the devices were obtained using HP4155C semiconductor parameter analyzer.

3. RESULT AND DISCUSSION

The crystal structure of the zinc silicate film was investigated by X-ray diffraction with Cu Kα radiation. Figure 1 presents a series of XRD patterns of sample before and after annealing at 1,000℃. Before annealing, the broad diffraction peaks for ZnO only were observed in Fig. 1(a). According to the JCPDS data card no. 36-1451, diffraction peaks at 31.7°, 33.8°, 36.04°, 47.24°, 56.01°, 62.09°, 67.26°, and 70.2° correspond to (100), (002), (101), (102), (110), (103), (112), and (004) planes of ZnO, respectively. In Fig. 1(b), the diffraction peaks for annealed Zn_2SiO_4 films were observed. According to the JCPDS data card no. 37-1485, diffraction peaks at 22.18°, 25.55°, 31.6°, 34.05°, 38.9°, 49.02°, and 65.75° correspond to (300), (220), (113), (410), (223), (333), and (173) planes of Zn_2SiO_4, respectively.

In this annealing condition, the grain size of Zn_2SiO_4 film was about 52 nm, calculated from the full-width at half maximum (FWHM) of the Zn_2SiO_4 (410) peak (at 2θ≈34.05°) by using the

$$D = \frac{k\lambda}{\beta \cos\theta} \quad (1)$$

Scherrer's formula.

where D is the crystallite size, k was Scherrer's constant = 0.9, λ=1.5406 Å (X-ray wavelength), and ß was FWHM of XRD peak. It matches well with result of SEM measurement. Referring to XRD patterns, we observed that Zn_2SiO_4 film is formed by annealing process at 1,000℃ for 1 or 5 hours.

Figure 2 shows SEM and AFM image of sample before and after annealing at 1,000 ℃. After annealing process, we observed that about 300 nm size of grains and 50 nm size of nanocrystals were formed separately. Unknown atoms agglomerated to form grain walls of ~20 nm height, which were measured by AFM. In SEM measurement, grain size of small particle is about 50 nm. Referring to calculated grain size from XRD patterns, we concluded that the nanocrystals are Zn_2SiO_4.

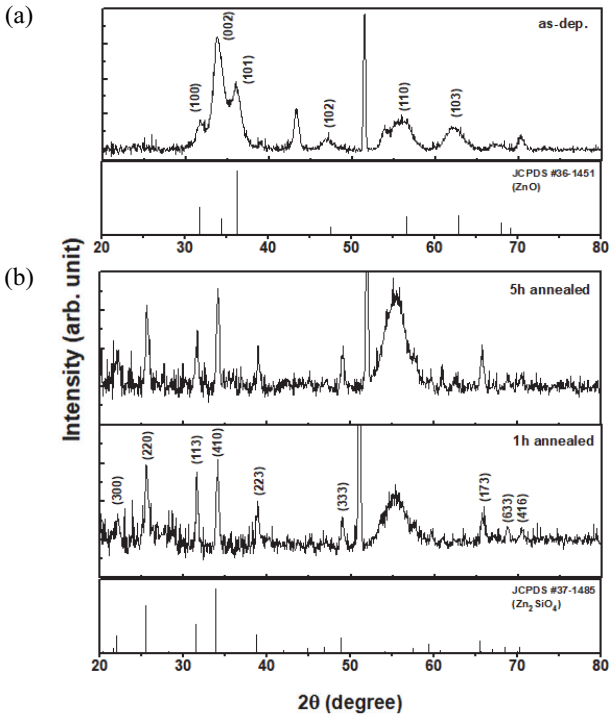

Fig. 1. XRD patterns of (a) as-deposited and (b) annealed ZnO and SiO_2 mixed film [the standard XRD pattern for ZnO (JCPDS #36-1451) and Zn_2SiO_4 (JCPDS #37-1485) is given at bottom for comparison].

The typical I-V characteristics were measured by a two point contact method through a current-voltage sourcemeter. The positive voltage sweep is defined as the current flow from the top to the bottom electrodes. Figure 3 shows the I-V curves of the unipolar resistive switching in the device. A forming voltage of 6 V was required for the reproducible resistive switching process in a new sample. The resistance of the forming process is lower than that of the HRS because of the forming of the conducting filaments in the $ZnSiO_x$ layer. During a low-magnitude positive voltage sweep the rapid decrease in the current (reset) appeared at about 1 V. This means the resistive state of the device changed from the LRS

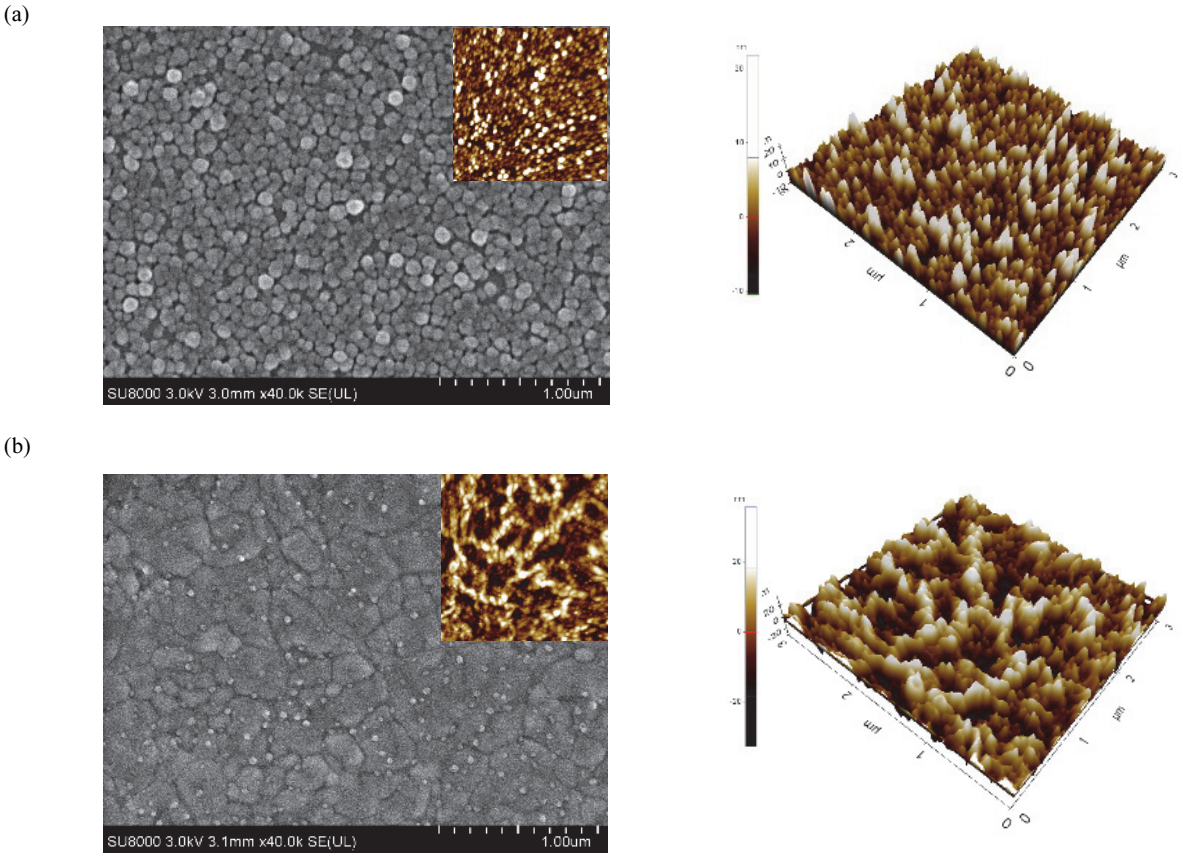

Fig. 2. SEM and AFM images of $ZnSiO_x$ film (a) before and (b) after annealing process.

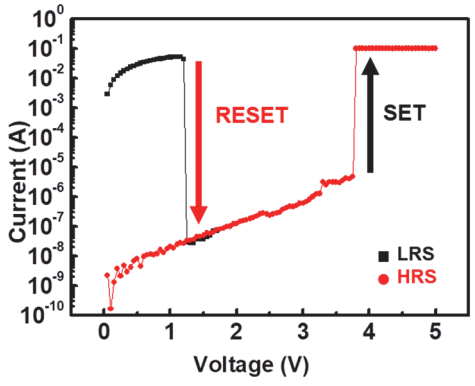

Fig. 3. I-V characteristics for the unipolar resistive switching in Ag/$ZnSiO_x$/highly doped n-type Si substrate devices.

to the HRS. When a high-magnitude positive voltage sweep was continuously applied to the device again, an abrupt increase in the current (set) was measured at about 4 V. That is, the resistive state of the device switched from the HRS to the LRS.

Figure 4 presents the electrical endurance property over 50 switching cycles in the $ZnSiO_x$ device. We observed unipolar resistive switching characteristics over 50 switching cycles. The currents in the LRS and HRS were measured at 0.5 V in each dc voltage sweep after forming process. The average current ratio between the HRS and LRS was about 10^6. The currents in the HRS were well suppressed to about 10^{-9} A at 0.5 V (readout voltage) after the annealing process with the co-sputtered $ZnSiO_x$ films.

In order to understand the conduction mechanism of the HRS and LRS, we analyzed the fitting data of I-V curves according to the equation for the Schottky emission and Ohm's law. Figure 5(a) presents the plot of the Schottky emission for the HRS which indicates that *log*J increases linearly with $E^{1/2}$. The dominant conduction in the Schottky emission for the HRS comes from the thermally-activated electrons which are injected over the conduction band of the oxide from the metal [14]. Schottky barrier and trap depth should be reduced as increasing applied electrical field. After

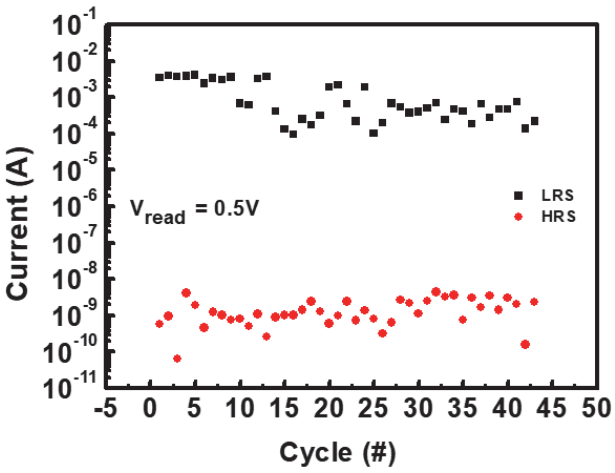

Fig. 4. The electrical endurance property over 50 switching cycles in the $ZnSiO_x$ device is presented (the currents in the LRS and HRS were measured at 0.5 V in each dc voltage sweep after forming process).

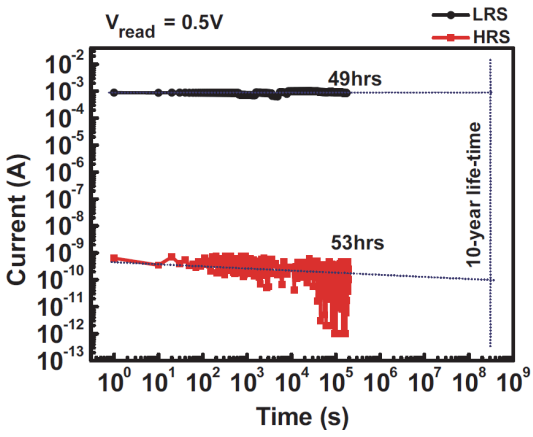

Fig. 6. The time-dependent retention properties are measured in the LRS and HRS under the readout voltage of 0.5 V [the retention in the LRS is more stable relative to those in the HRS and is long enough with no obvious on-off ratio degradation along the repeated reading process, even widened (>10^5 sec)].

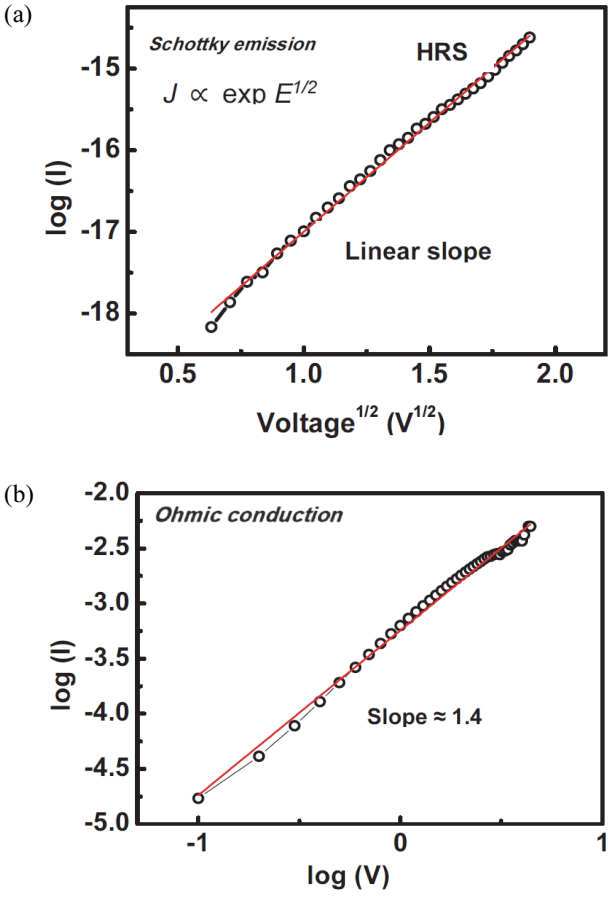

Fig. 5. (a) I-V curve for the HRS: the plot of the Schottky emission indicates that *log* J increases linearly with $E^{1/2}$ and (b) I-V curve for the LRS: the plot shows an Ohmic conduction behavior with a slope of ~1.4.

set process, conductive filament paths are formed inside the oxide, which indicates the LRS. As shown in Fig. 5(b), the double logarithmic plot of I-V curves gives a slope of about 1 for the low voltage region less than 0.5 V. The dominant conduction mechanism for the LRS is Ohmic conduction along conductive filament paths. The Schottky emission and Ohm' law are consistent with the predictions of a filament model that explains the resistance change by the formation and rupture of the conductive filaments.

Figure 6 shows the retention properties of the zinc silicate devices, which are measured in their LRS and HRS under the readout voltage of 0.5 V. The time-dependent retention in the LRS is more stable relative to those in the HRS and maintain obviously large resistance ratio (~10^6) for over 10^5 sec.

4. SUMMARY

The resistive switching characteristics of $ZnSiO_x$, zinc silicate film, based metal-insulator-metal (MIM) devices has been investigated. $ZnSiO_x$ thin film was prepared by co-sputtering method and the post annealing process was performed for 1 hour at 1,000℃. Referring to XRD patterns, we observed that ZnO and SiO_2 combined to $ZnSiO_x$ film by annealing process. SEM and AFM images of $ZnSiO_x$ thin film before and after annealing at 1,000℃ were obtained. After annealing process, we observed that about 300 nm size of

grains and 50 nm size of nanocrystals were formed separately. The new zinc silicate thin films exhibited unipolar resistive switching properties which are reproducible over 50 switching cycles and long retention (~10^5 sec) without degradation shown in Fig. 6. After the electro-forming process, Zn metallic filaments are created in the zinc silicate layer. The observed unipolar resistive switching is caused by the repetition process of the rupture/recreation of Zn metallic filaments. Out-diffused Zn in the zinc silicate film contributes to the formation of these metallic filaments [15]. Through the results of I-V curves and fittings, the conduction mechanisms were explained by using Ohmic conduction for the LRS and Schottky emission for the HRS. The average value of the resistance ratio between the HRS and the LRS was about ~10^6 when the readout voltage was 0.5 V. The currents in the HRS were well suppressed to about 10^{-9} A at 0.5 V (readout voltage) after the annealing process.

ORCID

Junghyun Sok https://orcid.org/0000-0002-8250-0433

ACKNOWLEDGEMENT

This work was supported by the 2021 sabbatical year research grant of the University of Seoul.

REFERENCES

[1] T. W. Hickmott, *J. Appl. Phys.*, **33**, 2669 (1962). [DOI: https://doi.org/10.1063/1.1702530]

[2] J. F. Gibbons and W. E. Beadle, *Solid-State Electron.*, **7**, 785 (1964). [DOI: https://doi.org/10.1016/0038-1101(64)90131-5]

[3] G. Dearnaley, A. M. Stoneham, and D. V. Morgan, *Rep. Prog. Phys.*, **33**, 1129 (1970). [DOI: https://doi.org/10.1088/0034-4885/33/3/306]

[4] J. G. Simmons, *J. Phys. D: Appl. Phys.*, **4**, 613 (1971). [DOI: https://doi.org/10.1088/0022-3727/4/5/202]

[5] A. Sawa, *Mater. Today*, **11**, 28 (2008). [DOI: https://doi.org/10.1016/S1369-7021(08)70119-6]

[6] T. C. Chang, K. C. Chang, T. M. Tsai, T. J. Chu, and S. M. Sze, *Mater. Today*, **19**, 254 (2016). [DOI: https://doi.org/10.1016/j.mattod.2015.11.009]

[7] F. M. Simanjuntak, D. Panda, K. H. Wei, and T. Y. Tseng, *Nanoscale Res. Lett.*, **11**, 368 (2016). [DOI: https://doi.org/10.1186/s11671-016-1570-y]

[8] H. Wang, C. Zou, L. Zhou, C. Tian, and D. Fu, *Microelectron. Eng.*, **91**, 144 (2012). [DOI: https://doi.org/10.1016/j.mee.2011.05.037]

[9] A. Beck, J. G. Bednorz, Ch. Gerber, C. Rossel, and D. Widmer, *Appl. Phys. Lett.*, **77**, 139 (2000). [DOI: https://doi.org/10.1063/1.126902]

[10] S. Q. Liu, N. J. Wu, and A. Ignatiev, *Appl. Phys. Lett.*, **76**, 2749 (2000). [DOI: https://doi.org/10.1063/1.126464]

[11] B. J. Choi, A.B.K. Chen, X. Yang, and I. W. Chen, *Adv. Mater.*, **23**, 3847 (2011). [DOI: https://doi.org/10.1002/adma.201102132]

[12] H. Jiang, X. Y. Li, R. Chen, X. L. Shao, J. H. Yoon, X. Hu, C. S. Hwang, and J. Zhao, *Sci. Rep.*, **6**, 22216 (2016). [DOI: https://doi.org/10.1038/srep22216]

[13] B. W. Fowler, Y. F. Chang, F. Zhou, Y. Wang, P. Y. Chen,. F. Xue, Y. T. Chen, B. Bringhurst, S. Pozder, and J. C. Lee, *RSC Adv.*, **5**, 21215 (2015). [DOI: https://doi.org/10.1039/C4RA16078A]

[14] K. H. Jung, S. G. Song, K. W. Park, J. H. Sok, K. M. Kim, and Y. S. Park, *J. Korean Phys. Soc.*, **70**, 489 (2017). [DOI: https://doi.org/10.3938/jkps.70.489]

[15] J. Kim, A. I. Inamdar, Y. Jo, H. Woo, S. Cho, S. M. Pawar, H. Kim, and H. Im, *ACS Appl. Mater. Interfaces*, **8**, 9499 (2016). [DOI: https://doi.org/10.1021/acsami.5b11781]